Suppression of spirals and turbulence in inhomogeneous excitable media

Jiang-Xing Chen,[1,2,*] Jun-Wen Mao,[2,3] Bambi Hu,[2,4] Jiang-Rong Xu,[1] Ya-Feng He,[2] Yuan Li,[1] and Xiao-Ping Yuan[1]
[1]*Department of Physics, HangZhou Dianzi University, Hangzhou 310018, China*
[2]*Department of Physics, Centre for Nonlinear Studies, and The Beijing-Hong Kong-Singapore Joint Centre for Nonlinear and Complex Systems (Hong Kong), Hong Kong Baptist University, Kowloon Tong, Hong Kong, China*
[3]*Department of Physics, HuZhou Teachers College, HuZhou 313000, China*
[4]*Department of Physics, University of Houston, Houston, Texas 77204-5005, USA*
(Received 30 October 2008; published 22 June 2009)

Suppression of spiral and turbulence in inhomogeneous media due to local heterogeneity with higher excitability is investigated numerically. When the inhomogeneity is small, control tactics by boundary periodic forcing (BPF) is effective against the existing spiral and turbulence. When the inhomogeneity of excitability is large, a rotating electric field (REF) is utilized to "smooth" regional heterogeneity based on driven synchronization. Consequently, a control approach combining BPF with REF is proposed to suppress the spiral and turbulence. The underlying mechanism of successful suppression is discussed in terms of dispersion relation.

DOI: 10.1103/PhysRevE.79.066209 PACS number(s): 82.40.Bj, 82.40.Ck, 47.54.−r, 87.19.Hh

I. INTRODUCTION

Rotating spiral wave is one of the most typical two-dimensional patterns in excitable media, such as the cardiac tissue [1], neural tissue [2], Belousov-Zhabotinsky (BZ) and surface reactions [3,4], and slime mold colonies [5]. It is conjectured that spiral waves and their instability are involved in causing certain types of cardiac arrhythmia such as ventricular tachycardia and fibrillation [1,6–9].

The stability of propagating wave in inhomogeneous media has attracted much attention in the past decades, since many natural biological excitable media are heterogeneous [10–14]. For example in the cardiac tissue, anatomical obstacles may break electrical waves with consequent spiral waves and turbulence [15–19]. In the presence of inhomogeneity, various methods to suppress spiral and turbulence have been put forward [19–24]. Up to now, most documented studies have concentrated on inhomogeneous media with obstacles which are treated as non(sub)-excitable or non(sub)-diffusive regions, since this kind of heterogeneity resulting from ischemia, fibrosis, and sarcoidosis in cardiac tissue is frequently encountered in practice. However, the inhomogeneity in biological excitable tissues is very complex [25]. Under certain conditions [25–29], the excitability in some local regions may be higher than that in other regions in the medium. This type of heterogeneity may also negatively affect the stability of propagating wave and bring deleterious effects, but it has not been studied so far, which makes the investigation worthwhile and meaningful.

II. MODEL

In this paper, the influence of regional heterogeneity with higher excitability is studied. We concentrate on control strategies to suppress spiral and turbulence in this type of medium. By changing the regional excitability in heterogeneity, we alter the degree of inhomogeneity of the medium. When the deviation of excitability between inside and outside the heterogeneity is small, boundary periodic forcing (BPF) will be applied. If the deviation is large, a combined control approach by utilizing a rotating electric field (REF), based on driven synchronization, is proposed. The mechanism underlying the control method is discussed.

We study the spatiotemporal dynamics of excitation in inhomogeneous excitable medium by means of a two-component FitzHugh-Nagumo-type model (the Bär model) describing the interaction of a fast activator u and a slow inhibitor v variable [30,31]:

$$\frac{\partial u}{\partial t} = \frac{1}{\varepsilon(x,y)} u(1-u)[u-(v+b)/a] + D\nabla^2 u + F(t),$$

$$\frac{\partial v}{\partial t} = g(u,v) - v, \tag{1}$$

where the function $g(u,v)$ takes the form $g(u)=0$, if $0 \le u < 1/3$; $g(u)=1-6.75u(u-1)^3$, if $1/3 \le u \le 1$; and $g(u)=1$, if $1<u$. $\varepsilon(x,y)$ describes the spatial distribution of excitability. In our simulation, a regional disk-shape domain with different excitability from surrounding regions is studied. The values ε_{in} and ε_{out} indicate the excitability inside and outside the disk, respectively:

$$\varepsilon(x,y) = \begin{cases} \varepsilon_{in}, R \le R_0 \\ \varepsilon_{out}, R_0 \le R. \end{cases} \tag{2}$$

Here R_0 is the radius of the disk, $R=\sqrt{(x_i-x_0)^2+(y_i-y_0)^2}$ with $(x_0,y_0)=(50.0,50.0)$ the coordinate of the central point of the disk and i, j the integer numbers which correspond to the discretized x and y variables as $x_i=(i-1)\Delta x$, $y_i=(j-1)\Delta y$, respectively. We fixed $a=0.84$, $b=0.07$, and $D=1.0$ to ensure that the system is an excitable medium [31]. Zero-flux boundary conditions have been employed. A spatial (temporal) discretization of $\Delta x=\Delta y=0.3906$ on a 256×256 array with fixed time step $\Delta t=0.02$ has been used in an explicit Euler scheme.

*jxchen@hdu.edu.cn

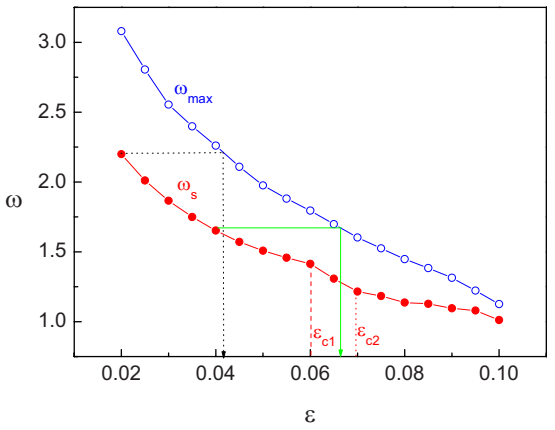

FIG. 1. (Color online) Open circles denote maximal frequencies $\omega_{\max}$ of one-dimensional wave trains as a function of ε. Full circles show rotating frequencies ω_s of spiral wave at each ε. Values are obtained from FFT method. Vertical line indicates the onset of meandering (dashed line) at ε_{c1} and spiral breakup (dotted line) at ε_{c2}. The horizontal dotted line from ω_s at $\varepsilon=0.02$ and curve of $\omega_{\max}$ shows a point of intersection at about $\varepsilon=0.042$. The horizontal solid line from ω_s at $\varepsilon=0.04$ and curve of $\omega_{\max}$ shows a point of intersection at about $\varepsilon=0.067$.

III. RESULTS AND DISCUSSION

In Fig. 1, we show the dispersion relation that gives a maximum frequency $\omega_{\max}$ at each ε (by shortening the one-dimensional ring supporting periodic wave trains to obtain the $\omega_{\max}$ [32]), i.e., $\omega_{\max}(\varepsilon)$ is a function of ε. From the phase portrait of this model [31], it is clear that the refractory period of the medium is determined by its excitability. If the frequency of periodic wave is larger than $\omega_{\max}$, one wave front will fall into the refractory back of its ahead wave. Thus, no periodic wave with frequency above $\omega_{\max}$ can exist since it exceeds the power of the excitable medium [33,34]. With suitable initial conditions, a homogeneous medium may exhibit various interesting spiral waves as ε is varied [31]. The frequency of spiral wave ω_s is also characterized by excitability of the medium [i.e., $\omega_s(\varepsilon)$] and will always be smaller than $\omega_{\max}$, which can been seen from Fig. 1. When $\varepsilon \in [0.02, 0.06]$, the system supports a stable periodic spiral wave. At $\varepsilon=0.06$, the system undergoes a Hopf bifurcation and a second modulate frequency is introduced [35,36]. The spiral wave becomes quasiperiodic and exhibits meandering behavior. Due to the pronounced Doppler effect, which leads to temporal frequency measured from the region near the spiral core across $\omega_{\max}$, the increase in value ε beyond $\varepsilon=0.071$ causes breakup of spiral [31,33,37]. The condition $\varepsilon_{in} > \varepsilon_{out}$ means that the heterogeneity is a "defect" that may occur at anatomic source-sink mismatches, such as papillary or pectinate muscle insertions, or when excitability is depressed regionally due to ischemia or drugs [38]. The influences of this kind of defect on propagating wave have been investigated intensively [10–19,23,24]. In the case of $\varepsilon_{in} < \varepsilon_{out}$, the excitability inside the disk ($R < R_0$) is higher than that in other regions, forming a "hot" disk.

We concentrate on the dynamical behaviors and control strategies in inhomogeneous medium with $\varepsilon_{in} < \varepsilon_{out}$. In Fig. 2(a), we show a turbulence state in the presence of a hot disk. In such a case, the deviation of excitability between the regions between inside and outside the disk domain is small ($\Delta\varepsilon=\varepsilon_{out}-\varepsilon_{in}=0.01$). With the evolution of time, one can see that a small spiral is spontaneously generated in the disk [see Fig. 2(b)]. The small spiral grows into the outer region that possesses lower excitability [see Fig. 2(c)]. Eventually, the medium is occupied by a well developed single spiral [see Fig. 2(d)]. From Fig. 2(e), it is clearly shown that the temporal frequency from excitable point outside the disk [$\omega_s(\varepsilon_{out})$] is increased to that of the inside spiral [$\omega_s(\varepsilon_{in})$] at about $t=300$, that is, from $\omega_s(\varepsilon_{out})=1.87$ to $\omega_s(\varepsilon_{in})=2.19$. This phenomenon can be rationalized by the dispersion relation in Fig. 1. Developed spiral inside the disk [$\varepsilon_{in}=0.02$ with corresponding $\omega_s(\varepsilon_{in})=2.19$, see Fig. 1] possesses higher frequency than that of surrounding turbulence [$\varepsilon_{out}=0.03$ with corresponding $\omega_s(\varepsilon_{out})=1.87$]. As a principle in competition of waves, high-frequency wave will wipe away

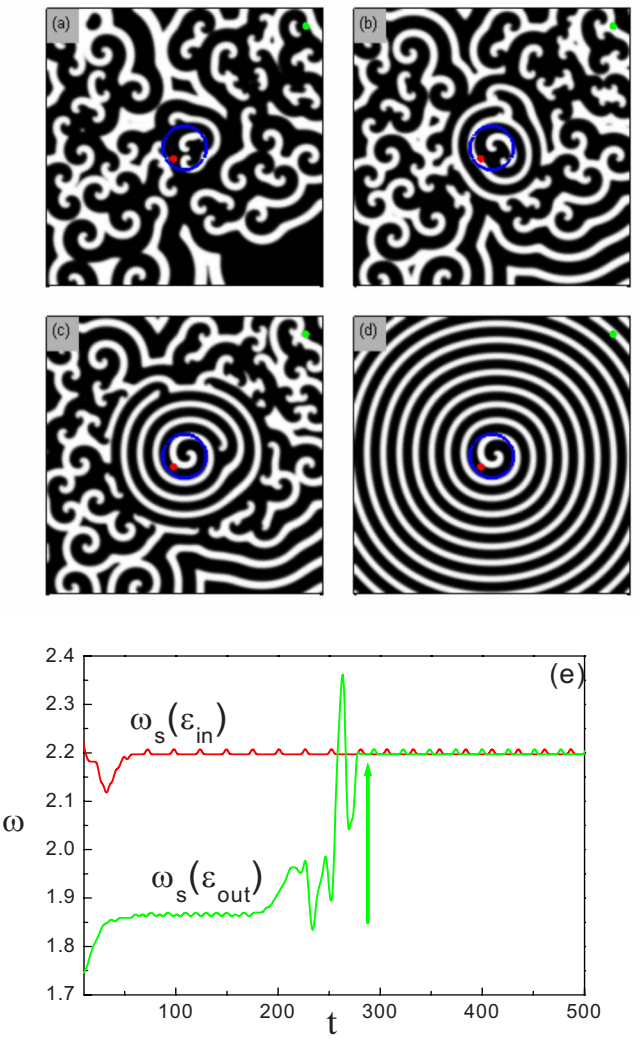

FIG. 2. (Color online) Development of turbulence in inhomogeneous medium possessing hot disk schematically indicated by the superimposed circle with $R_0=5.0$, $\varepsilon_{in}=0.02$, $\varepsilon_{out}=0.03$ at (a) $t=10$, (b) $t=50$, (c) $t=100$, and (d) $t=500$. (e) The evolution of temporal frequency at points (118,118) (dot inside the disk) and (240,240) (dot outside the disk), respectively.

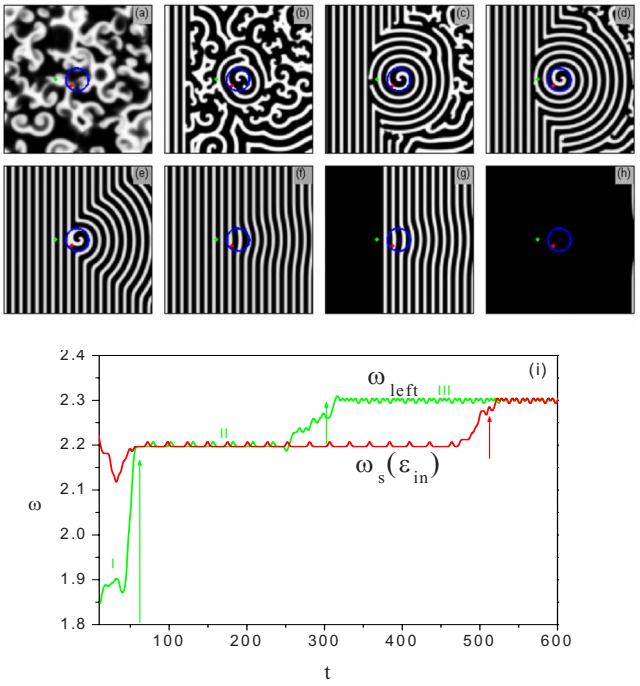

FIG. 3. (Color online) Suppression of spiral and turbulence by applying BPF with $F=2.0$ and $\omega_F=2.30$ at (a) $t=0$, (b) $t=50$, (c) $t=150$, (d) $t=200$, (e) $t=500$, (f) $t=1000$, (g) $t=1020$, and (h) $t=1050$. (i) The evolution of temporal frequency at points (118,118) on the inside the disk showed by the $\omega_s(\varepsilon_{in})$ curve and (90,128) on the left of the disk showed by the ω_{left} curve, respectively. Other parameters: $\varepsilon_{in}=0.02[\omega_s(\varepsilon_{in})=2.19]$ and $\varepsilon_{out}=0.03[\omega_s(\varepsilon_{out})=1.87]$. The labels I, II, and III in the ω_{left} curve show three different dynamical regimes with time evolution.

low-frequency wave [19,24,39,40]. Therefore, the turbulence is suppressed by the coming spiral from the disk. Thus, the emergence of a "hot" region may act as local pacing source to terminate the turbulence. Since the local hot region is possible to be realized in cardiac muscle, we put forward an imaginary view that one can utilize this effect to take action in the complex process of cardiac arrhythmia.

A. Suppression by BPF

To eliminate the spiral and turbulence, a method of BPF will be proved to be effective. In Fig. 3, we apply a BPF $F(t)=F\cos(\omega_F t)$ located at the left boundary strip at $x=0$. At the same time, spiral wave grows spontaneously from the disk [see Fig. 3(b)]. After the plane wave and the spiral meet [in Fig. 3(c)], they compete with each other. Gradually, the plane waves wipe away the spiral [see the process from Figs. 3(c)–3(f)]. Finally, the medium is occupied by the plane wave from the left boundary. When we switch off the BPF, the system approaches the desired rest state [see Figs. 3(g) and 3(h)].

A necessary condition of local pacing method to effectively suppress turbulence is that the principle of wave competition should be fulfilled, namely, the pacing frequency must be higher than that of the spiral and turbulence [19,24,39,40]. In Fig. 3, the frequency of BPF is $\omega_F=2.3$, that is to say, the principle works since $\omega_F>\omega_s(\varepsilon_{in})>\omega_s(\varepsilon_{out})$. Thus, both turbulence surrounding the disk and the spontaneous spiral from the disk can be suppressed. From the evolution of frequencies in selected points inside and outside the disk, one can see that they are both increased to the value $\omega_F=2.3$ [see Fig. 3(e)]. The frequency from the point inside the disk is increased from $\omega_s(\varepsilon_{in})=2.19$ to $\omega_F=2.3$ at about $t=520$ when the disk is invaded by the plane wave from left boundary. A point (90,128) is selected on the left of the disk. There are two jumps of frequency plotted from (90,128) (see the curve of ω_{left}): the first jump at about $t=50$, from $\omega_s(\varepsilon_{out})=1.87$ to $\omega_s(\varepsilon_{in})=2.19$, indicates occupation by growing spiral wave from the disk; while the second jump at about $t=320$, from $\omega_{out}=2.19$ to $\omega_{in}=2.3$, denotes that the previous spiral in this point is suppressed and conquered by the plane waves from left boundary finally.

Next, we fix the excitability inside the disk at $\varepsilon_{in}=0.02$ and decrease the excitability outside the disk (by increasing ε_{out}). The larger the value $\Delta\varepsilon=\varepsilon_{out}-\varepsilon_{in}$, the hotter and more inhomogeneous the heterogeneity will be. Our simulations show that a phenomenon such as that in Figs. 2(a)–2(d) cannot occur any longer when ε_{out} is increased across a critical value about 0.042, From Figs. 4(a)–4(d), one can see that a small spiral is spontaneously developed in the disk. However, the small spiral is restricted in the disk and cannot spread to other regions to suppress the turbulence, although its frequency is higher than that of the surrounding turbulence $[\omega_s(\varepsilon_{in})=2.19$ while $\omega_s(\varepsilon_{out})=1.57]$. Figure 4(e) displays independent frequency between the regions inside and outside the disk, showing insulated and block dynamical behavior and coexistence of different patterns with independent frequency in a medium, which also has been studied in Refs. [6,29].

To suppress the turbulence state, we apply the control method of BPF again. However, this method does not work in this time, no matter what values of amplitudes and frequencies of BPF are chosen. A typical example is shown in Figs. 5(a)–5(f). The plane wave from the left boundary can wipe away the turbulence on the left of the disk, with consequent increase in frequencies [see the curve ω_{left} in Fig. 5(g)]. However, the spiral in the disk and the turbulence on the right of the disk cannot be suppressed even after long time evolution, as shown in Figs. 5(b) and 5(c) and corresponding temporal frequency in Fig. 5(g). After we switch off the BPF, the waves from the disk and turbulence on the right of the disk invade into the left part [see Figs. 5(d)–5(f)]. Thus, the medium evolves into turbulence again.

The underlying reason for the two phenomena, i.e., the spiral from the disk cannot suppress turbulence and the plane wave generated by BPF cannot wipe away the existing turbulence, is attributed to the restriction of frequency characterized by dispersion relation. In order to successfully suppress existing waves or turbulence by generating new waves, two factors should be fulfilled. One is that the frequency of the new wave generated by BPF (with frequency ω_F) should be higher than that of the existing waves (ω_s), as a principle mentioned above. The other is that the frequency of the generated new waves cannot be higher than $\omega_{\max}(\varepsilon_{out})$, which is the capability of the medium at fixed ε_{out}. That is to say, the frequency of the produced new wave (ω_F) should fall into

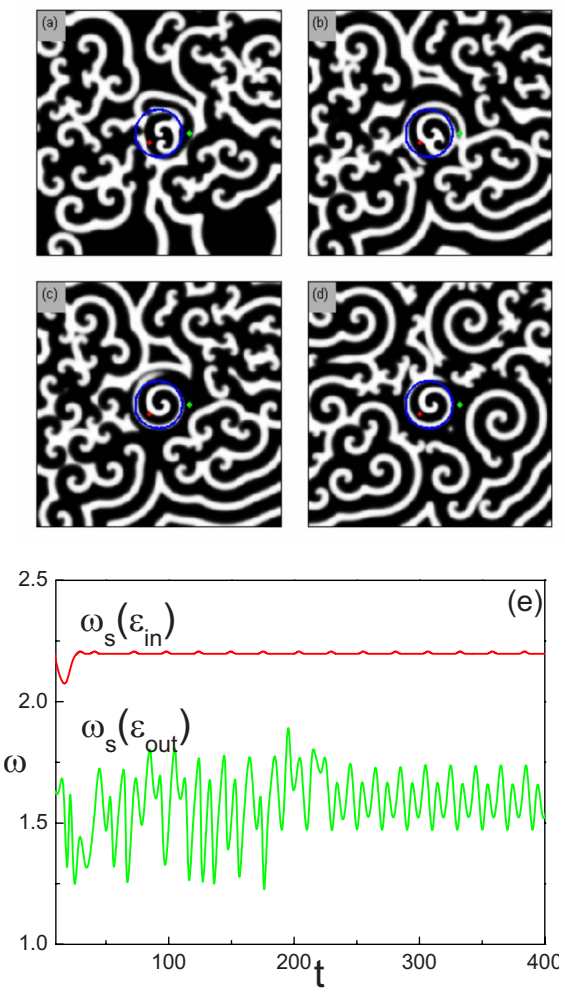

Fig. 4

FIG. 4. (Color online) Evolution of turbulence in inhomogeneous medium at (a) $t=10$, (b) $t=20$, (c) $t=60$, and (d) $t=2000$. Other parameters: $R_0=5.0$, $\varepsilon_{in}=0.02$, $\varepsilon_{out}=0.045$, $\omega_s(\varepsilon_{in})=2.19$, and $\omega_s(\varepsilon_{out})=1.57$ (obtained from FFT method). (e) Temporal frequency of points (118,118) on the inside and (160,128) outside the disk, respectively.

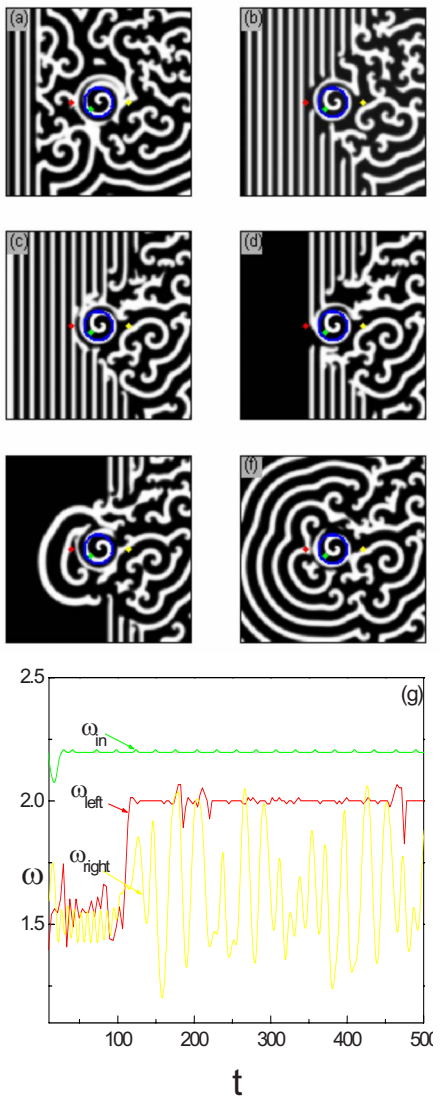

FIG. 5. (Color online) System at different time moments (a) $t=50$, (b) $t=200$, (c) $t=1000$, (d) $t=1020$, (e) $t=1040$, and (f) $t=1200$. The BPF with $F=2.0$, $\omega_F=\omega_{\max}(\varepsilon_{out})=2.10$ is switched off after $t=1000$. Other parameters are the same as that in Fig. 4. (g) Temporal frequency of points (90,128) on the left ω_{left}, inside (118,118) ω_{in}, and right (128,170) ω_{right} the disk.

the domain between ω_s and $\omega_{\max}(\varepsilon_{out})$ at fixed ε, i.e., $\omega_s < \omega_F < \omega_{\max}$. It is easy to find this region in Fig. 1. The frequency of spiral wave in the disk $[\omega_s(\varepsilon_{in})=2.19$ at $\varepsilon_{in}=0.02]$ determines the maximal ε_{out}. From the intersection of the horizontal dotted line and the curves of $\omega_{\max}$ in Fig. 1, we find a maximal value of ε_{out} at about 0.042, which is consistent with simulation result. Beyond $\varepsilon_{out}=0.042$, the corresponding value of $\omega_{\max}(\varepsilon_{out})$ is smaller than $\omega_s(\varepsilon_{in})=2.19$ in the disk with $\varepsilon_{in}=0.02$, i.e., $\omega_s(\varepsilon_{in}) > \omega_{\max}(\varepsilon_{out})$, which brings the result that the medium outside the disk cannot support spontaneous new wave from the disk with so high frequency. That is why the spiral from the disk cannot suppress surrounding turbulence when ε_{out} is increased beyond 0.042. In order to suppress the spiral in the heterogeneous disk and turbulence, the frequency of the BPF should be higher than that of the developed spiral in the disk, that is, $\omega_F > \omega_s(\varepsilon_{in})$. However, when ε_{out} goes beyond 0.042, this condition cannot be achieved since frequency of plane wave by BPF cannot approach the value higher than $\omega_{\max}(\varepsilon_{out})$ at fixed ε_{out} [19,41]. That is to say, $\omega_F < \omega_{\max}(\varepsilon_{out}) < \omega_s(\varepsilon_{in})$. Therefore, it is difficult to suppress the spiral turbulence in medium with this kind of hot disk.

B. Suppression by BPF in conjunction with REF

Thus, to control turbulence in medium with large deviation of excitability $\Delta\varepsilon$, the central problem is to decrease the frequency of the spontaneous spiral wave in the hot disk. Electric fields are known to have pronounced effects on behaviors of spiral waves [30,42–46]. Applying two ac electric fields perpendicular to each other with phase difference $\phi=\phi_y-\phi_x=\pi/2$ or $3\pi/2$, one can get a REF: $\mathbf{E}=(E_x,E_y)$

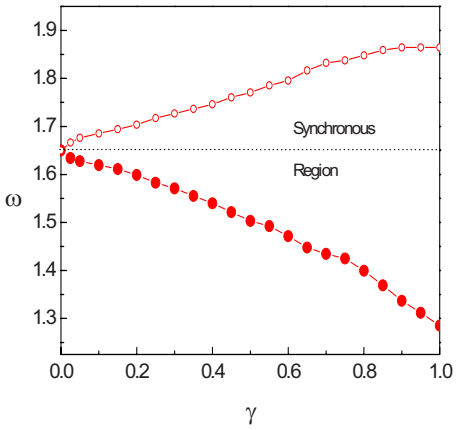

FIG. 6. (Color online) Synchronous diagram. The full (open) circles present the synchronized minimal (maximal) frequency of spiral at $\varepsilon_{in}=0.04$ induced by REF. The horizontal dot line indicates the frequency of spiral without control.

$=\gamma\cos(\omega t+\phi_x)\mathbf{i}+\gamma\cos(\omega t+\phi_y)\mathbf{j}$ [30]. A notable characteristic of the REF is that the direction of the electric field vector rotates while the amplitude is kept at a constant value. In light that both the REF and the spiral waves possess rotation symmetry, we make use of the REF to decrease the frequency of spontaneous spiral wave in the disk as our control strategy, basing on the driven synchronization. Correspondingly, the model can be modified:

$$\frac{\partial u}{\partial t}=\frac{1}{\varepsilon(x,y)}u(1-u)[u-(v+b)/a]+D\nabla^2u+M_u\mathbf{E}\cdot\nabla u+F(t),$$

$$\frac{\partial v}{\partial t}=g(u,v)-v+M_v\mathbf{E}\cdot\nabla v, \tag{3}$$

where $M_u=1$ and $M_v=0$. Other parameters have the same values as those in the original model (1).

Synchronization of spatially extended systems of oscillators to an external periodic forcing realizes a drive-response configuration, which has attracted a great deal of attention in recent studies [47–49]. Compared with most reported interesting synchronization driven by scalar external forcing [47–49], rotating spiral wave synchronized by a global vector REF is also a very attractive phenomenon. Now, we apply REF [with the same rotating direction as the spontaneous spiral in the disk, $\varepsilon_{in}=0.04$ with corresponding $\omega_s(\varepsilon_{in})=1.65$] on the medium to explore the driven synchronization. The frequency of REF is around that (ωs) of the spiral in the disk. The synchronous region of spiral in the disk induced by REF is displayed in the $\omega-\gamma$ plane in Fig. 6, showing so-called Arnold tongue of the 1:1 synchronization [50]. In the synchronous region, the frequency of rotating spiral can be synchronized to be equal to that of the REF. Note that the REF with opposite direction to the spiral cannot induce synchronization and may lead to complex motion based on the

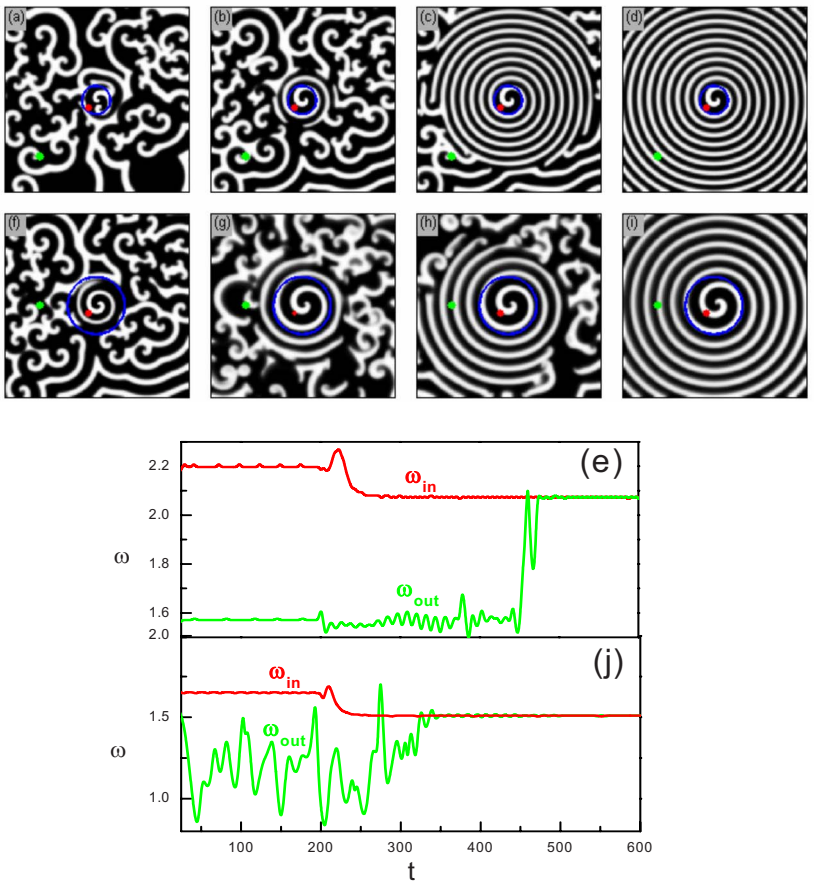

FIG. 7. (Color online) Two typical processes show suppression of turbulence by spiral wave which has been synchronized by the REF. Upper row: $\varepsilon_{in}=0.02$, $\varepsilon_{out}=0.045$, and $R_0=5.0$. Parameters of the REF: $\omega_F=2.07$ and $\gamma=0.5$. (a) $t=10$, (b) $t=180$, (c) $t=500$, and (d) $t=1000$. Lower row: $\varepsilon_{in}=0.04$, $\varepsilon_{out}=0.075$, and $R_0=10.0$. Parameters of the REF: $\omega_E=1.51$ and $\gamma=0.5$. (f) $t=20$, (g) $t=300$, (h) $t=400$, (i) $t=1000$. (e,j) The corresponding evolution of temporal frequency at points inside and outside the disk. (e) Point (118,118) inside and (50,50) outside the disk, (j) point (118,118) inside and (50,128) outside the disk.

forcing frequency and amplitude. Increasing the amplitude of REF strengthens the coupling between the spiral and REF, which broadens the region of synchronization. Since the synchronization occurs just around the frequency of spontaneous spiral in the disk while the deviation of frequency between inside and outside the disk is large now, the influences of REF to the surrounding turbulence can be neglected when driven synchronization occurs. We focus on the minimal frequency of spiral wave synchronized by REF with different amplitudes, which has been emphatically highlighted in Fig. 6.

The reduction in frequency of spiral in the disk makes the REF suitable to be a control method. In the upper row of Fig. 7, the excitability is $\varepsilon_{in}=0.02$ and $\varepsilon_{out}=0.045$. Without control, the dynamical behavior of system has been described in Fig. 4. In order to ensure the spiral wave grows into the region outside the disk, it is clearly indicated in Fig. 1 that the frequency of the spontaneous spiral in the disk should be decreased. After the REF with $\gamma=0.5$ and $\omega_E=2.07$ is switched on the system at $t=200$, the spiral in the disk invades into the region surrounding the disk and suppresses the spiral turbulence [see Figs. 7(a)–7(c)]. Ultimately, the medium is occupied by a single spiral [see Fig. 7(d)]. From evolution of corresponding temporal frequency of the point (118,118) on the inside and point (50,50) outside the disk in Fig. 7(e), one can see the effects induced by the REF. The frequency of the point (118,118) in the disk is decreased obviously after the REF is applied at $t=200$, from $\omega_s(\varepsilon_{in})=2.19$ to $\omega_E=2.07$, which shows a corresponding down jump in the $\omega_s(\varepsilon_{in})$ curve. Consequently, the spiral invades into the turbulence resulting in an upward jump of frequency at point (50,50) in the turbulence [see $\omega_s(\varepsilon_{out})$ curve].

In Figs. 7(f)–7(i), we give another example with $\varepsilon_{in}=0.04$, $\omega_s(\varepsilon_{in})=1.65$, and $\varepsilon_{out}=0.075$ (accordingly, $\omega_s(\varepsilon_{out})=1.18$, $\omega_{\max}(\varepsilon_{out})=1.525$, see Fig. 1). In this case, simulation shows that beyond the permitted value of $\varepsilon_{out}=0.067$ the outer region cannot support the wave coming from the disk, which agrees with the analysis in Fig. 1. Here $\varepsilon_{out}=0.075$ is larger than 0.067, namely, $\omega_s(\varepsilon_{in})=1.65$ is bigger than $\omega_{\max}(\varepsilon_{out})=1.525$. Therefore, the $\omega_s(\varepsilon_{in})$ should be dropped to the value lower than $\omega_{\max}(\varepsilon_{out})$. Then, we apply an REF with $\omega_E=1.51$ and $\gamma=0.5$ on the system. Note that $\omega_E=1.51$ is smaller than the $\omega_{\max}(\varepsilon_{out})=1.525$. Indeed, the spiral in the disk is synchronized by the REF accompanied with the decrease in frequency from 1.65 to 1.51, which gives rise to a consecutive single spiral in the medium [see the process in Figs. 7(f)–7(i)]. From the corresponding change in frequency in Fig. 7(j), one can also observe that the $\omega_s(\varepsilon_{in})$ is synchronized by REF with down jump of frequency from 1.65 to 1.51 at about $t=200$. Subsequently, $\omega_s(\varepsilon_{out})$ shows an upward jump from 1.18 to 1.51 indicating the coming of the central spiral.

Although the driven synchronization does not smooth the large inhomogeneity of excitability, it opens a way to turbulence control. Due to the reduction in frequency of spiral in the disk, BPF can be used again to suppress the turbulence. Consider the system described in Figs. 7(f)–7(i), the frequency of BPF should be larger than that of the REF (now, the spiral in disk is synchronized by REF) and smaller than the maximal frequency of medium outside the disk, i.e., ω_E

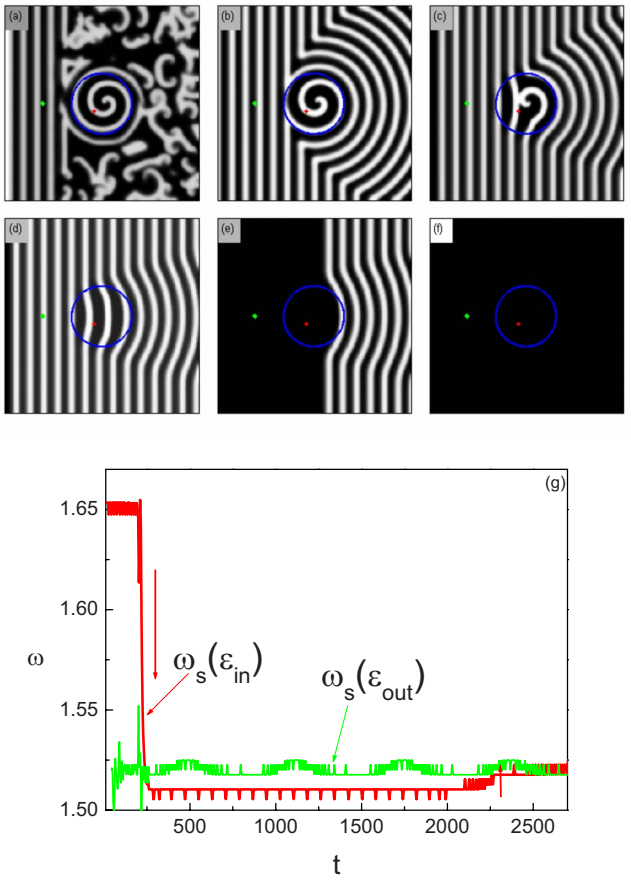

FIG. 8. (Color online) Spatial contour patterns of u under the combined control BPF+REF at different time moments. (a) $t=200$, (b) $t=1000$, (c) $t=2500$, (d) $t=4000$, (e) $t=4030$, (f) $t=4060$. $\omega_F=1.52$, $F=2.0$, $\omega_E=1.51$, and $\gamma=0.5$ are amplitudes and frequencies of BPF and the REF, respectively. The REF is switched off after $t=4000$. (g) The temporal frequency of points (50,128) on the outside and (118,118) inside the disk. Other parameters are the same as that in Figs. 7(e)–7(h).

$<\omega_F<\omega_{\max}(\varepsilon_{out})$. We select $\omega_F=1.52$ to fulfil the condition [$\omega_E=1.51$ and $\omega_{\max}(\varepsilon_{out})=1.525$]. Successfully, the turbulence and spiral are suppressed, which can be observed from the evolution of patterns in Figs. 8(a)–8(d). After switching off the BPF at $t=4000$, a rest state can be achieved ultimately. One can see this process in Figs. 8(e) and 8(f). In Fig. 8(g), the driven synchronization of spiral in the disk by the REF displays the first down jump in the $\omega_s(\varepsilon_{in})$ curve at about $t=250$; the second upward jump indicates the coming of plane wave from left boundary. The fluctuation of $\omega_s(\varepsilon_{out})$, due to the global periodic REF, does not influence the effect of control.

From the minimum frequency in the $\omega-\gamma$ synchronous plane and the dispersion relation in Fig. 1, we plot the maximal value ε_{out} at different amplitude of REF in Fig. 9 ($\varepsilon_{in}=0.04$ is fixed). The region "I" denotes that the turbulence outside the disk within the range $\varepsilon_{out}\in[0.04,0.067]$ can be suppressed by BPF. The region "II" indicates that both the spiral wave in the disk and the turbulence surrounding the disk can be suppressed by the combined method BPF+REF. $\varepsilon\uparrow$ shows the increased maximal value of $\varepsilon_{out}=0.092$ with

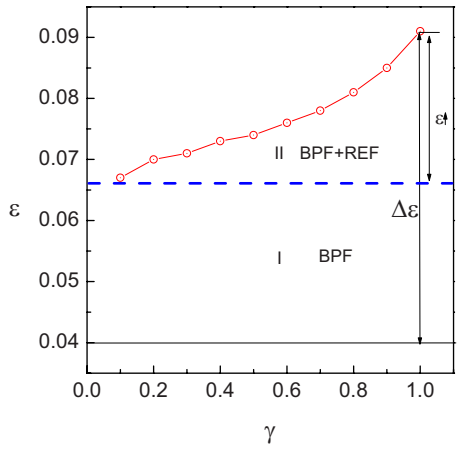

FIG. 9. (Color online) Open circles show the maximal values of ε_{out} beyond which combined control method BPF+REF cannot work when $\varepsilon_{in}=0.04$ is fixed. The region "I" denotes that the spiral turbulence can be suppressed by BPF when the deviation of excitability is small. The region "II" indicates the suppression of spiral turbulence can be achieved by BPF+REF when deviation of excitability is large.

$\gamma=1.0$. Under the control of REF, the deviation of excitability $\Delta\varepsilon$ between inside and outside the disk is increased from 0.027 (0.067–0.04) to 0.052 (0.092–0.04).

IV. CONCLUSION

In conclusion, we have studied the dynamical behaviors and control strategies in medium with inhomogeneous excitability. When the deviation of excitability in inhomogeneous medium is small, that is $\omega_s(\varepsilon_{out})<\omega_s(\varepsilon_{in})<\omega_{\max}(\varepsilon_{out})$, the property of the system is dominated by wave from the regions with higher excitability. In this case, the BPF is proved to be effective to suppress spiral turbulence. When the excitability in the heterogeneity is so large that $\omega_s(\varepsilon_{in})>\omega_{\max}(\varepsilon_{out})$, the dynamical property of medium is different. It seems that the dynamical behavior in different region is insulated. The control method of BPF no longer works due to the existence of wave in high excitable region and the following wake turbulence. By applying an REF possessing rotation symmetry, the frequency of the spiral wave in high excitable region can be decreased via driven-synchronization. Based on the synchronization, the waves in the medium can be successfully suppressed by BPF with suitable frequency.

The complex tissues under various conditions make the spatial distribution of different excitability possible in nature. Consequently, various spatiotemporal patterns with independent frequencies may coexist in different regions with different excitability. It is possible to observe those complicated states, including coexistence of multiple spirals with independent frequencies, coexistence of regular waves (target, spiral, etc.) and turbulence separated by insulated regions, and even more complicated coexistence of patterns. Since REF is spatially uniform, it can efficiently "smooth" the inhomogeneity of excitability in different regions and consequently change the interaction of coexisted waves. As a potential control method, local and low-amplitude pacing of defibrillation of cardiac tissue has attracted much attention. Thus, although our results are obtained in a simple excitable model, we believe the combined method by BPF+REF may contribute to control dynamics in various inhomogeneous media such as cardiac systems, neural network systems, and BZ reaction.

ACKNOWLEDGMENTS

We would like to thank Professor Gang Hu for useful discussions. This work was supported by the National Nature Science Foundation of China (Grants No. 10747120 and No. 10847113) and Natural Science Foundation of Zhejiang Province (Grant No. Y607525).

[1] J. M. Davidenko, A. V. Pertsov, R. Salomonsz, W. Baxter, and J. Jalife, Nature (London) **355**, 349 (1992); F. X. Witkowski, L. J. Leon, P. A. Penkoske, W. R. Giles, M. L. Spano, W. L. Ditto, and A. T. Winfree, *ibid.* **392**, 78 (1998).
[2] N. A. Gorelova and J. Bureš, Neurobiology **14**, 353 (1983).
[3] A. T. Winfree, Science **175**, 634 (1972); V. K. Vanag and I. R. Epstein, *ibid.* **294**, 835 (2001).
[4] S. Jakubith, H. H. Rotermund, W. Engel, A. von Oertzen, and G. Ertl, Phys. Rev. Lett. **65**, 3013 (1990).
[5] N. Nishiyama, Phys. Rev. E **57**, 4622 (1998).
[6] A. T. Winfree, Science **266**, 1003 (1994).
[7] R. A. Gray *et al.*, Science **270**, 1222 (1995); R. A. Gray, A. M. Pertsov, and J. Jalife, Nature (London) **392**, 75 (1998).
[8] A. V. Panfilov and P. Hogeweg, Science **270**, 1223 (1995); Phys. Rev. E **53**, 1740 (1996).
[9] L. Glass, Phys. Today **49** (8), 40 (1996).
[10] G. Bub, L. Glass, N. G. Publicover, and A. Shrier, Proc. Natl. Acad. Sci. U.S.A. **95**, 10283 (1998); G. Bub, A. Shrier, and L. Glass, Phys. Rev. Lett. **88**, 058101 (2002); B. E. Steinberg, L. Glass, A. Shrier, and G. Bub, Philos. Trans. R. Soc. London, Ser. A **364**, 1299 (2006).
[11] F. Xie, Z. Qu, A. Garfinkel, and J. N. Weiss, Am. J. Physiol. **280**, 535 (2001).
[12] A. M. Zhabotinsky, M. D. Eager, and I. R. Epstein, Phys. Rev. Lett. **71**, 1526 (1993).
[13] D. Pazó, L. Kramer, A. Pumir, S. Kanani, I. Efimov, and V. Krinsky, Phys. Rev. Lett. **93**, 168303 (2004).
[14] I. Schebesch and H. Engel, Phys. Rev. E **57**, 3905 (1998).
[15] K. Agladze, J. P. Keener, S. C. Müller, and A. Panfilov, Science **264**, 1746 (1994).
[16] Z. Nagy-Ungvarai, A. M. Pertsov, B. Hess, and S. C. Müller, Physica D **61**, 205 (1992).
[17] A. M. Pertsov, A. V. Panfilov, and F. U. Medvedeva, Biofizika **28**, 100 (1983).
[18] J. Jalife, Annu. Rev. Physiol. **62**, 25 (2000).
[19] Y. Q. Fu, H. Zhang, Z. Cao, B. Zheng, and G. Hu, Phys. Rev.

E **72**, 046206 (2005).
[20] For a recent review, see A. S. Mikhailov and K. Showalter, Phys. Rep. **425**, 79 (2006).
[21] S. Takagi, A. Pumir, D. Pazó, I. Efimov, V. Nikolski, and V. Krinsky, Phys. Rev. Lett. **93**, 058101 (2004).
[22] A. Pumir, V. Nikolski, M. Hörning, A. Isomura, K. Agladze, K. Yoshikawa, R. Gilmour, E. Bodenschatz, and V. Krinsky, Phys. Rev. Lett. **99**, 208101 (2007).
[23] J. Schlesner, V. S. Zykov, H. Brandtstädter, I. Gerdes, and H. Engel, New J. Phys. **10**, 015003 (2008).
[24] G. N. Tang, M. Y. Deng, B. Hu, and G. Hu, Phys. Rev. E **77**, 046217 (2008).
[25] C. Antzelevitch, S. Sicouri, S. H. Litovsky, A. Lukas, S. C. Krishnan, J. M. D. Diego, G. A. Gintant, and D. W. Liu, Circ. Res. **69**, 1427 (1991).
[26] J. Haverinen and M. Vornanen, J. Exp. Biol. **209**, 549 (2006); R. M. Shaw and Y. Rudy, Circ. Res. **81**, 727 (1997).
[27] C. G. Nichols, E. N. Makhina, W. L. Pearson, Q. Sha, and A. N. Lopatin, Circ. Res. **78**, 1 (1996).
[28] N. A. Dimitrova and G. V. Dimitrov, Biol. Cybern. **66**, 185 (1991).
[29] F. G. Xie, Z. Qu, J. N. Weiss, and A. Garfinkel, Phys. Rev. E **63**, 031905 (2001); R. Cassia-Moura, F. G. Xie, and H. A. Cerdeira, Int. J. Bifurcation Chaos Appl. Sci. Eng. **14**, 3363 (2004); J. X. Chen, J. R. Xu, X. P. Zhang, J. W. Zhang, and X. W. Zhang, Cent. Eur. J. Phys. **7**, 108 (2009).
[30] J. X. Chen, H. Zhang, and Y. Q. Li, J. Chem. Phys. **124**, 014505 (2006).
[31] M. Bär and M. Eiswirth, Phys. Rev. E **48**, R1635 (1993).
[32] W. Jahnke and A. T. Winfree, Int. J. Bifurcat. Chaos **1**, 445 (1991).
[33] Q. Ouyang, H. L. Swinney, and G. Li, Phys. Rev. Lett. **84**, 1047 (2000).
[34] A. Belmonte and J. M. Flesselles, Phys. Rev. Lett. **77**, 1174 (1996).
[35] G. Li, Q. Ouyang, V. Petrov, and H. L. Swinney, Phys. Rev. Lett. **77**, 2105 (1996).
[36] D. Barkley, M. Kness, and L. S. Tuckerman, Phys. Rev. A **42**, 2489 (1990); D. Barkley, Phys. Rev. Lett. **68**, 2090 (1992).
[37] H. Zhang, J. X. Chen, Y. Q. Li, and J. R. Xu, J. Chem. Phys. **125**, 204503 (2006).
[38] J. N. Weiss, Z. Qu, P. S. Chen, S. F. Lin, H. S. Karagueuzian, H. Hayashi, A. Garfinkel, and A. Karma, Circulation **112**, 1232 (2005).
[39] Y. Kuramoto, *Chemical Oscillations, Waves, and Turbulence* (Springer-Verlag, Berlin, 1984).
[40] H. Zhang, Z. Cao, N. J. Wu, H. P. Ying, and G. Hu, Phys. Rev. Lett. **94**, 188301 (2005).
[41] S. Rüdiger, E. M. Nicola, J. Casademunt, and L. Kramer, Phys. Rep. **447**, 73 (2007).
[42] O. Steinbock, J. Schütze, and S. C. Müller, Phys. Rev. Lett. **68**, 248 (1992).
[43] K. I. Agladze and P. De Kepper, J. Phys. Chem. **96**, 5239 (1992).
[44] A. P. Muñuzuri, M. Gómez-Gesteira, V. Pérez-Munuzuri, V. I. Krinsky, and V. Pérez-Villar, Phys. Rev. E **50**, 4258 (1994).
[45] V. Krinsky, E. Hamm, and V. Voignier, Phys. Rev. Lett. **76**, 3854 (1996).
[46] J. J. Taboada, A. P. Muñuzuri, V. Pérez-Muñuzuri, M. Gómez-Gesteira, and V. Pérez-Villar, Chaos **4**, 519 (1994).
[47] V. Petrov, Q. Ouyang, and H. L. Swinney, Nature (London) **388**, 655 (1997); A. L. Lin, M. Bertram, K. Martinez, H. L. Swinney, A. Ardelea, and G. F. Carey, Phys. Rev. Lett. **84**, 4240 (2000); V. K. Vanag, L. Yang, M. Dolnik, A. M. Zhabotinsky, and I. R. Epstein, Nature (London) **406**, 389 (2000).
[48] For a recent review, see S. Boccaletti, J. Kurths, G. Osipov, D. L. Valladares, and C. S. Zhou, Phys. Rep. **366**, 1 (2002).
[49] O. Steinbock, V. Zykov, and S. C. Müller, Nature (London) **366**, 322 (1993); V. Zykov, O. Steinbock, and S. C. Müller, Chaos **4**, 509 (1994).
[50] J. X. Chen, H. Zhang, and Y. Q. Li, J. Chem. Phys. **130**, 124510 (2009).